Tests of a Grazing-Incidence Ring Resonator Free-Electron Laser

David H. Dowell, Mary L. Laucks, A. R. Lowrey, John L. Adamski, Denis J. Pistoresi, Donald R. Shoffstall, Melvin Paul Bentz, Richard H. Burns, Jay Guha, Kenneth C. Sun, William Tomita, A. H. Lumpkin, S. C. Bender, D. Byrd, and Robert L. Tokar

Abstract—**The Boeing free-electron laser (FEL) optical cavity has been changed from a simple concentric cavity using two spherical mirrors to a larger grazing-incidence ring resonator. The new resonator consists of two mirror telescopes located at each end of the wiggler with a round-trip path length of approximately 133 m. Each telescope is a grazing-incidence hyperboloid followed by a normal-incidence paraboloid. Initial tests showed that poorly positioned ring focus and unreliable pointing alignment resulted in reduced and structured FEL output. (First lasing operation occurred on March 23 and 24, 1990.) Later efforts concentrated on improving the resonator alignment techniques and lowering the single-pass losses. FEL performance and reliability have significantly improved due to better ring alignment. The alignment procedure and recent lasing results are described. The effect the electron beam has on lasing is also discussed. Measurements are presented showing how FEL temporal output and wavelength are sensitive to electron beam energy variations.**

I. Introduction and Description of an FEL

THIS paper describes operational experience of the first free-electron laser using a grazing-incidence ring resonator. Previously, the Boeing and Los Alamos Visible-Wavelength Free-Electron Laser Experiment had successfully demonstrated operation of a concentric-cavity free-electron laser (FEL). Measurements gave extraction efficiencies up to 0.75%, demonstrating good trapping and deceleration in a 4% tapered wiggler [1]. However, during this experiment there was already evidence of optical damage to the spherical end mirrors.

Essentially, all FEL's have used the simple concentric design for their optical cavities, and many have experienced some form of damage to the resonator optics [2]. Therefore, it is important in developing FEL's to investigate other optical cavity designs tolerant of high optical intensities [3]. This paper's motivation is to test the feasibility of a grazing-incidence ring resonator on a FEL. The use of a high-incidence angle with beam-expanding optics significantly increases the damage threshold.

The Boeing and Los Alamos FEL optical cavity was changed from a simple concentric cavity using two spherical mirrors to a larger grazing-incidence ring resonator [3], [4]. The new resonator was designed to test the design and operation of a grazing-incidence optical cavity for a high-power FEL. The experiment has successfully operated a FEL with a ring-resonator optical cavity. This was especially challenging because the FEL was operated at visible wavelengths. This paper describes a study of using a ring resonator as the optical cavity in a FEL, from both viewpoints of electron beam quality and ring-resonator alignment.

The ring resonator was installed in Spring 1988 and fine alignment began in Autumn 1989. Preliminary electron beam tests were done in December 1989 and February 1990 and showed that irregular mechanical movement of the outcoupler made determination of the proper cavity length difficult. Resonator losses were also large because the ring's focus was downstream of the wiggler, rather than at the center. This focus error caused the optical beam to be clipped by the wiggler vacuum tube, which is 4.7 mm in diameter and 5 m long. Work was initiated to correct these problems. The outcoupler was fixed, the ring refocused, and the optics cleaned during the period from mid-February to mid-March. Resumed electron beam testing gave much improved operation, and the ring successfully lased March 23–24, 1990.

However, after this initial success, lasing was unreliable and the FEL output exhibited considerable temporal structure. Measurements were made to distinguish between electron beam and ring-resonator effects. By May 1990, it became evident that the method for aligning the ring resonator was insufficient. A FELEX [5] model calculation showed that startup would be difficult with a misaligned resonator but should not "structure" the output [6], [7]. Here, structured output means a temporal oscillation in the outcoupled power, where the FEL starts from noise, approaches saturation, shuts off, and restarts several times during the 100 μs long macropulse.

Because of these difficulties, two optical diagnostics were added to the ring resonator during June and July 1990. These were a sampling mirror viewed by a camera

Manuscript received April 15, 1991; revised August 2, 1991. This work was supported by the U.S. Army Strategic Defense Command under Contract DASG60-87-C-0011.

D. H. Dowell, M. L. Laucks, A. R. Lowrey, J. Adamski, D. Pistoresi, and D. R. Shoffstall are with Boeing Aerospace and Electronics, Seattle, WA 98124.

M. P. Bentz, R. H. Burns, J. Guha, K. Sun, and W. Tomita are with Rocketdyne Division of Rockwell International, Canoga Park, CA 91305.

A. H. Lumpkin, S. Bender, D. Byrd, and R. L. Tokar are with the Los Alamos National Laboratory, Los Alamos, NM 87545.

IEEE Log Number 9103646.

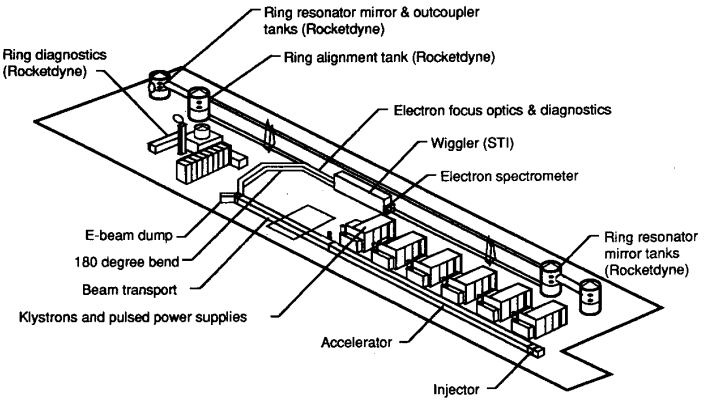

Fig. 1. Overview of the Boeing free-electron laser facility.

TABLE I
ELECTRON BEAM, THUNDER WIGGLER, AND RING RESONATOR DESIGN PARAMETERS

Electron Beam	
Electron beam energy	110 MeV
Repetition rate	2 Hz
Macropulse length	110 μs
Micropulse spacing	443 ns
Emittance ($4\epsilon_{rms}$)	100-120 π mm mR
Macropulse energy jitter	0.5%-0.75% FWHM
Micropulse energy spread	0.5% FWHM
Micropulse width	12 ps FWHM
Micropulse charge	3 nC
Thunder Wiggler	
Length	5 m in 10, 50 cm sections
Wiggler period	2.18 cm
Number of periods	220 periods
Peak magnetic field	10.2 KG
Wiggler parameter	1.8 (peak)
Wiggler parameter	1.31 (rms)
Betatron period	5.6 m
Taper	0% (during these tests)
Ring Resonator	
Ring Rayleigh range	240 cm
Hyperboloid focal length	−105 cm
Paraboloid focal length	698 cm
Telescope magnification	7×
Hyperboloid-paraboloid spacing	600 cm
Round-Trip path length/time	133 m/443 ns

connected to a video digitizer to quantify the location of the ring resonator's focus accurately, and a pulsed-alignment laser beam sampled by pellicles viewed by gated-intensified cameras to ensure that the round-trip optical beams overlapped. This instrumentation was integrated into the operation of the FEL and significantly improved reliability and lasing output. This paper describes these changes along with an analysis of some results from these FEL experiments.

An overview of the Boeing FEL is given in Fig. 1. The FEL design parameters are listed in Table I. The accelerator has been discussed in [8]. Beamline and instrumentation upgrades have been necessary to achieve enough gain for lasing [9]. The ring resonator is contained in the vacuum tanks located at each end of the wiggler and is described in Section II. An account of some of the ring resonator optical measurements is found in [10] and [11]. Section III presents the early lasing test results. Section IV gives an analysis of these experiments and presents improved lasing performance due to better alignment techniques for the ring resonator. Section V reviews the experimental results.

II. THE RING RESONATOR OPTICAL CAVITY

The optical resonator optics are contained in four large vacuum tanks, two at each end of the wiggler (Fig. 1). The ring resonator design parameters are given in Table I; Fig. 2 shows the ring resonator in detail. The ring optics consists of a beam-expanding Galilean telescope at the downstream wiggler end, followed by an identical reducing Galilean telescope upstream of the wiggler. The beam-expanding hyperboloid mirror at grazing incidence has a negative focal length of 105 cm. This mirror is followed by a paraboloid with a 698 cm focal length. The beam in the resonator's return leg is collimated.

It is important to realize the outcoupler transmission depends strongly on wavelength to suppress the generation of wavelength sidebands. Its transmission as a function of wavelength is shown in Fig. 3. The ring losses due to the other mirrors is approximately 25%, so it is necessary to keep the lasing wavelength below 630 nm to keep the total loss below 30%. Approximately 9% of this loss is attributed solely to a high spatial frequency ripple across the hyperboloid surfaces [12] that scatters light out of the optical mode. The remaining losses result from using bare silicon hyperboloids for these initial tests instead of the silver-coated mirrors and from longitudinal astigmatism and alignment errors that lead to clipping the optical mode at the wiggler [10]. Later tests were to use the silver-coated optics and correct the astigmatism.

The ring-resonator alignment is established using two helium-neon (HeNe) lasers. One is injected into the ring

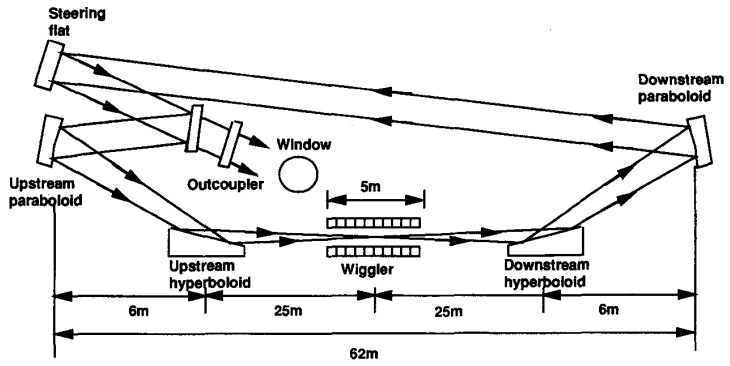

Fig. 2. Grazing-incidence ring resonator.

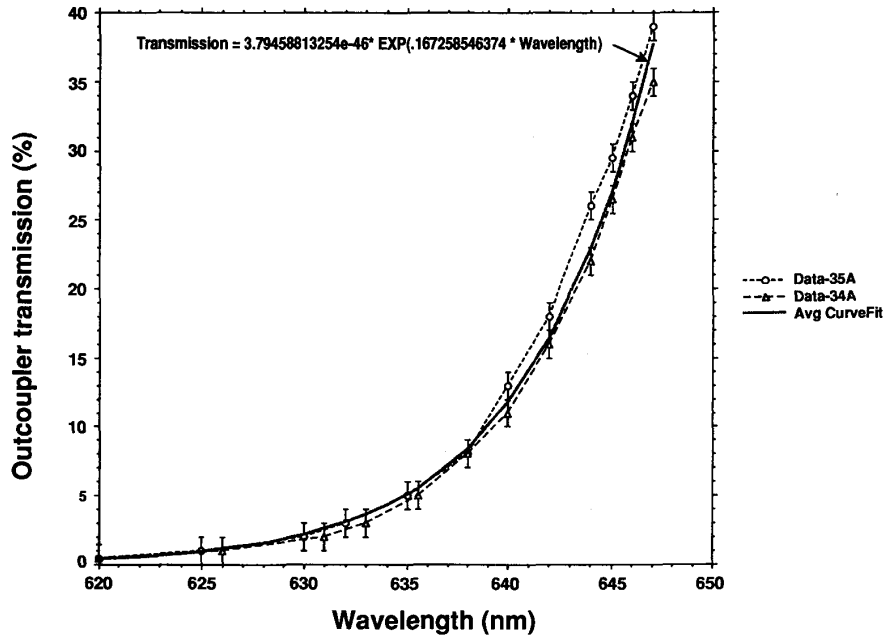

Fig. 3. Outcoupler transmission versus wavelength.

using a hologram, while the second uses an optical pellicle. The hologram beam is discussed here and the pellicle-injected multipass beam is described in Section IV.

A. Hologram Beam

Fig. 4 illustrates the hologram beam injection system that produces both forward and reverse propagating beams. ("Forward" is in the same direction as the FEL optical beam.) Both beams are mode matched to the resonator and are produced by the same hologram by retroreflecting the injection laser beam back through the same hologram. A second hologram is used to pick off a piece of the forward round-trip for analysis by a self-referencing interferometer [4], [11]. This interferometer is useful for quantifying the various contributions to the wave front distortion from the ring resonator. The analyzed interferometric data provides the Zernike polynomial set necessary to model the FEL.

However, it turns out the interferometer is rather insensitive to the ring's focus location and pointing alignment. These are two important needs that the additional ring diagnostics provide. The reverse beam is turned out of the vacuum by a backward facing mirror to measure the focal properties of the ring [10]. This is also shown in Fig. 4. Measurements done after the first lasing tests of March and May showed that instead of the round-trip focus for a forward-going beam occurring near or at the wiggler center, the focus was at the wiggler's entrance. In particular, the measurements made in June indicated that the horizontal round-trip focus was 267 cm and the vertical focus was 192 cm upstream of the 5 m wiggler's center. This meant that the ring resonator was optically unstable during the March–May testing period. Since May, the

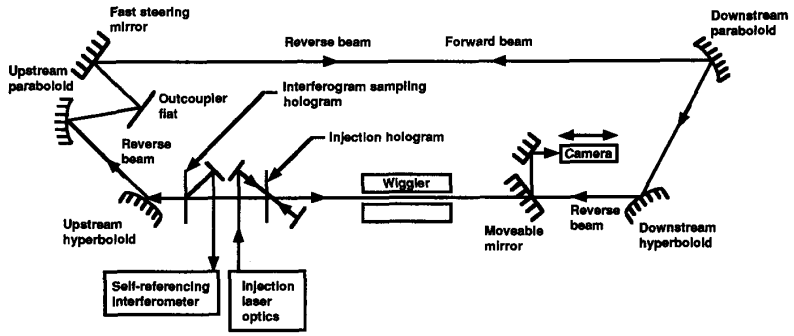

Fig. 4. Hologram alignment laser system.

downstream telescope spacing has been decreased to move the ring focus closer to the wiggler center [10].

B. Cavity Stabilization

Another consideration in the ring-resonator dynamics is the optical stabilization system [4], [10]. Stabilization is done by active feedback control of the fast-steering mirror using the signal from a quadcell located at the wiggler center. An off-axis laser begins near the wiggler center and circulates around the ring, returning to the quadrant detector on the opposite side of the wiggler. Unfortunately, the present control circuit is limited to frequencies below approximately 30 Hz. The remaining peak-to-peak amplitude of the optical beam motion is between 300 and 500 μm and has two frequency components, one near 50 Hz and the other near 100 Hz. A major vibration source is the beamline cryogenic vacuum pumps.

C. Concentric Cavity versus Ring Resonator

The startup difficulties can be understood from the ring's walking-mode characteristics. Ring-resonator walking behavior is compared with the concentric cavity in Fig. 5. The calculations give the pass-to-pass centroid motion at the wiggler. The vertical scales are in units of the beam waist size. The amplitude of the concentric cavity walk is similar to that of the ring resonator. The main distinction is that the concentric cavity oscillates slowly about the optical axis, whereas the ring jumps from side to side. This rapid pass-to-pass oscillatory pattern is what can make startup more difficult for the ring than the concentric configuration when the resonator is poorly aligned. If the initial optical beam position begins far off the optical axis in the concentric cavity, then the next few passes will return close to it. However, for the ring-resonator case, the next pass will occur just as far off on the opposite side of the optical axis and, having much less overlap with the electron beam (approximately 1 mm in diameter), reduce the chances for lasing.

Because of this walking behavior it was necessary to develop a technique to align the centroids of the pass-to-pass beams. This was done after the first lasing tests, and the improvement in reliability and extraction efficiency is described in Section IV.

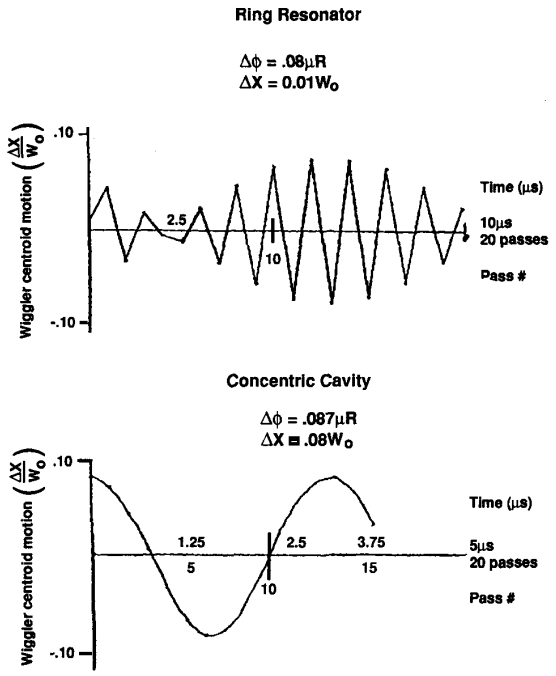

Fig. 5. Comparison of concentric cavity and ring resonator walking modes.

III. First FEL Tests

This section outlines the process of matching the electron beam to the wiggler and setting the cavity length in preparation for lasing. The last subsection gives lasing test results. The lasing tests discussed here occurred March 23–24, 1990 and May 3–4, 1990.

A. Electron Beam Matching, Alignment, and Diagnostics

Good electron beam quality at the wiggler is crucial for optimal lasing at visible wavelengths. After the beam is brought around the 180° bend onto the wiggler axis, its emittance and stability are measured. If the emittance is too large or has excessive transverse positional jitter, then usually the beam has not been sized or steered properly into the bend or accelerator, or the acceleration RF needs

adjusting. Some of these effects are described in [9]. Controling electron beam quality was a major issue during these tests.

The electron beam size and divergence are matched to the Thunder wiggler with the aid of a computer program that calls the TRANSPORT [13] electron beam optics code, retrieves quadrupole settings from the database, and uses results of two-screen emittance measurements. Once properly sized, the beam is allowed to drift into the wiggler and is viewed by the wiggler optical transition radiation (OTR) screens. Measurements of the beam size on the 11 wiggler screens placed every 50 cm (9 OTR and 2 alumina) confirm that the electron beam's diameter is constant along the wiggler [14].

The electron beam is aligned to the ring resonator optical axis using software generated marks on the video screen indicating the centroids of the alignment laser on each of the wiggler screens. The marks are done in software to allow for daily shifts in the camera mount positions and the resonator axis. This is also done for the screens in front of the wiggler. Steering correctors in the Thunder wiggler are used to steer the electron beam onto these alignment marks. The positioning accuracy is approximately ± 25 μm.

After passing through the wiggler, the electron beam is deflected by a magnetic spectrometer into a Faraday cup beam dump (see Fig. 1). The beam strikes a 300 μm thick, diamond-turned aluminum screen placed just in front of the Faraday cup. The OTR emission from this screen is brought out of the spectrograph's shielding using two fused-silica lenses that relay it to a gated, intensified CID camera. The gate on this camera can be varied in both duration and delay to measure the energy of a single micropulse or of groups of micropulses [9]. If the FEL extraction is greater than approximately 0.1%, then the lasing versus nonlasing centroid shift of the electron beam energy can be measured with this spectrometer to determine the interaction efficiency. This system is an improved version of that used during the concentric cavity tests [1], [15].

B. Setting the Cavity Length

For lasing to occur, the round-trip cavity length needs to match the electron micropulse spacing to within tens of microns. The technique for setting the cavity length involves viewing the light from the outcoupler with a streak camera, which is triggered to pick out one of the micropulses of light. If the round-trip length does not equal the pulse spacing, the streak image will show a primary optical pulse followed by smaller pulses offset in time. These smaller pulses are the ringdown light of optical echoes from the preceding electron beam pulses. The temporal spacing between these pulses gives the amount the cavity is out of synchronism with the electron beam. The relative amplitude of the ringdown pulses gives the losses from pass to pass. The upper inset in Fig. 6 shows streak camera ringdown data. The spacing between the optical pulses

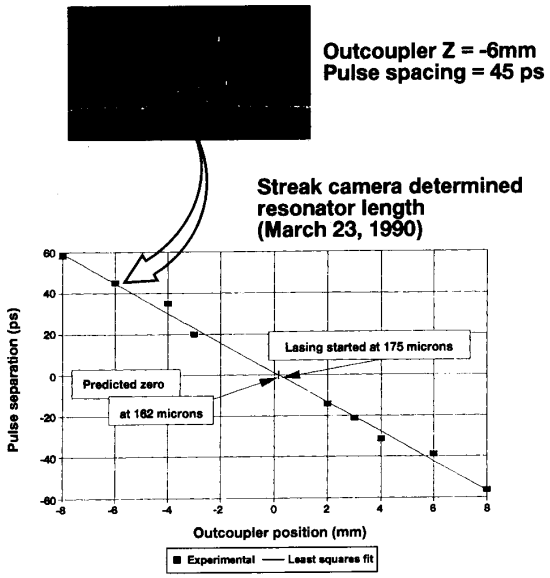

Fig. 6. Method for setting the ring-resonator cavity length.

is 45 ps corresponding to the ring-resonator round-trip path length being 13.5 mm shorter than the spacing between the electron beam micropulses. This is approximately twice the outcoupler's relative position because of the folded optical path between the fast steering mirror, outcoupler, and upstream paraboloid (see Fig. 2).

As mentioned earlier, the relative heights of these ringdown pulses reflect the single round-trip optical loss of the resonator. Obviously the loss should be the same between any two successive pulses. However, Fig. 6 (inset) shows irregular pass-to-pass loss. The observed loss is, successively, 70%, 30%, 70%, etc. This is caused by the outcoupled optical beam moving back and forth across the narrow slit of the streak camera in a manner identical to the side-to-side walking mode described in Section II. This kind of streak camera data serves as a tool for detecting relative misalignments between the electron beam and the ring resonator axis and should be developed further in future experiments.

Because the electron beam pulsewidth is 12 ps (FWHM), the ringdown light from the preceding pulse begins to merge with the direct pulse at about 3 mm (1 ps = 0.3 mm) away from the proper cavity length. Therefore, the pulsewidth limits the range for directly setting the cavity length. Determining the cavity length directly using the streak camera is accurate only if several ringdown pulses can be observed. In order to limit the search range to 100 μm, it would be necessary to observe at least out to the 20th ringdown pulse in the streak camera. Unfortunately, there is far from enough light remaining from 20 passes around the ring to make such a measurement.

Fig. 6 illustrates the method used to determine the proper cavity length. The temporal spacing of the direct and ringdown pulses are plotted versus the outcoupler's z position. This was done for positions out to 8 mm on either

side of the proper length. The data were then fit with a straight line to produce the expected outcoupler position at 162 μm. The outcoupler was then placed at 0 μm and stepped in 10 μm intervals while watching a photomultiplier tube (PMT) for some enhancement in the outcoupled light. When this was done on March 23, the ring began to lase at 175 μm. Since this occasion, the technique has correctly predicted the resonator length to ± 100 μm.

C. Early Lasing Test Results

The early lasing operation can be characterized as unreliable with fluctuating output. The first lasing operation done with the ring resonator was March 23, 1990. Saturation occurred over approximately 50 μs, or half the macropulse length. Fig. 7 shows an early measurement of the temporal structure for a typical macropulse. The output peaked twice at approximately 300 nJ per micropulse.

The May 1990 lasing intensity also exhibited strong temporal structure, as seen in Fig. 8. These four macropulses are interesting for both their differences and similarities. The peak energy is about the same, but the structure varies from pulse to pulse. However there are constant features in the output variations. For example, there is a sharp valley in the vacuum photodiode (VPD) output approximately 30 μs from the end of lasing. This valley is present in all four macropulses. The energy variation of the electron beam during the macropulse does not appear to be the cause. Another similarity is a common 10 μs or roughly 20-pass period in the outcoupled energy. This period is suggestive of the 17-pass walking mode described in Section II.

It is curious that the lasing stops when the electron beam energy is the flattest. A possible explanation would involve the nonisochronicity of the 180° bend. The nominal value is approximately 4.4 ps per percent of energy change. For the observed peak-to-peak energy slew of 0.25%, the micropulse spacing could change by about 1 ps or 300 μm. Because the cavity-length detuning curve is less than 100 μm wide, this is enough to lose longitudinal overlap and cause the lasing to stop. This effect was observed in FEL tests with the concentric cavity.

The wavelength was 627 nanometers (nm) with a 2 nm full width at half maximum (FWHM), shown in Fig. 9. Taking the ringdown loss to be 50%, the FEL extraction efficiency during the early lasing period was

$$\eta = \frac{E_\mu L_{\mathrm{RD}}}{T_{\mathrm{out}} E_{e\text{-beam}}} = 0.0036\%$$

where E_μ is the outcoupled energy per micropulse, T_{out} is the transmission of the outcoupler at 627 nm (as given by Fig. 3), L_{RD} is the ringdown loss, and $E_{e\text{-beam}}$ is the electron beam energy in each micropulse.

The conclusions of computer calculations [6] were that poor pointing alignment of the ring resonator would make startup difficult, but once lasing began the electron beam would dominate the FEL's output. How sensitive the FEL was to the electron beam characteristics would depend on the amount of excess gain the system had over the losses. Generally speaking, if the ratio of small-signal gain to single-pass loss was greater than two, the FEL would be relatively insensitive to variations in the electron beam. Of course, for the gain to be so high would require the

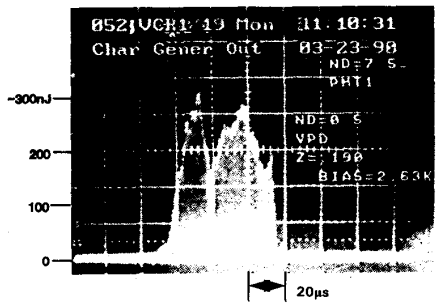

Fig. 7. Vacuum photodiode (VPD) measurement of optical macropulse during initial lasing tests.

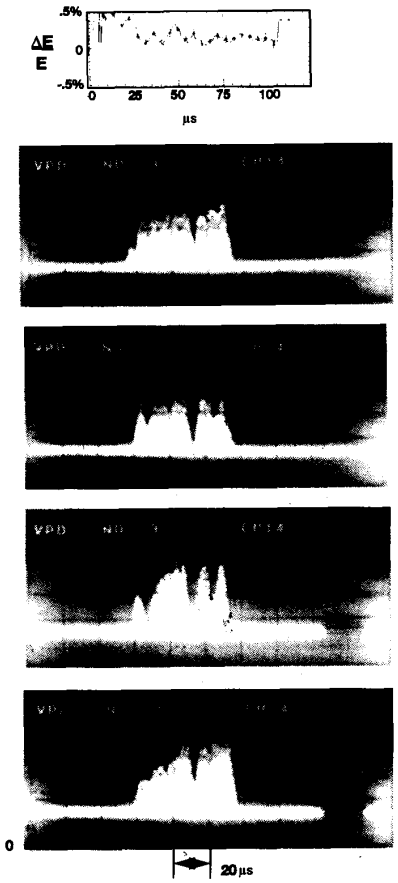

Fig. 8. Comparison of FEL intensity with electron beam energy slew and jitter.

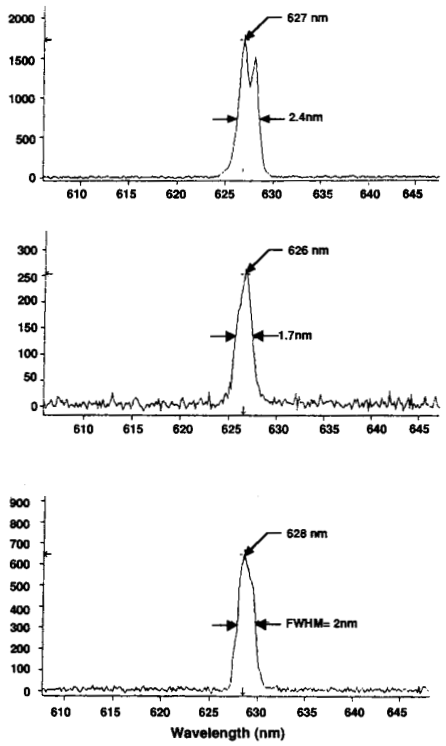

Fig. 9. Optical multichannel analyzer (OMA) spectra for three macropulses.

electron beam to be very stable during the macropulse. Experimentally, simply attaining startup remained the greatest difficulty, and the modeling indicated this was a resonator alignment problem. This was cured by installing additional resonator instrumentation and developing better procedures for operation. These instruments and subsequent lasing tests are described in the next section.

IV. Pass-to-Pass Ring Resonator Alignment and FEL Tests

This section reviews alignment procedures that corrected the overlap of the circulating optical beam and the general position of the resonator's focus. However, considerable astigmatism was still present during these tests. The process was to confirm more reliable and consistent operation with these system fixes and then to make a final correction to the resonator aberrations and stabilization system. The plan also included another round of upgrading the electron beam. Unfortunately, the direction of this FEL program changed and the ring-resonator experiment was discontinued. These are the final experimental results from these ring-resonator tests.

A. Pass-to-Pass Alignment

The effects described above clearly demonstrated the need for better experimental understanding of the ring's pass-to-pass alignment. Therefore, in addition to the hologram alignment laser, an additional alignment scheme was implemented. The layout for this laser system is shown in Fig. 10. A second laser is injected into the ring using a thin pellicle and is focused at the wiggler center. It can be aligned to the wiggler axis using the mirrors, M1 and M2. The beam is chopped at 2 Hz into 200 ns long pulses by a pockels cell located between the HeNe laser and a pinhole and lens combination. Two other pellicles, P1 and P2, located at each end of the wiggler can be inserted into the beamline to reflect a small portion of the injected laser light. The light from these sampling pellicles is directed into two gated, intensified CID cameras. Roughly 5% of the light from the downstream pellicle P2 is also reflected into a photomultiplier tube (PMT) to measure the ringdown losses.

A typical ringdown pulse train from the PMT is shown in Fig. 11. The 200 ns injected beam is the first pulse, followed by a series of successive pass pulses spaced at the 443 ns round-trip time of the ring. The round-trip ring losses are between 35 and 40% and exhibit a slight walking-mode effect.

The transverse positions of these various round-trip beams at the pellicle locations P1 and P2 are determined by the gated cameras. Adjusting the gate delay in 443 ns intervals (the ring round-trip time) allows the cameras to view up to the fourth round-trip beam before the light becomes too faint. Fig. 12 plots the centroid locations of the optical beam versus pass number around the ring. The positions are relative to the location of the injected beam. The observed pass-to-pass oscillatory motion mirrors the side-to-side oscillations calculated in Fig. 5, and is a large fraction of the 1 mm electron beam diameter.

Using this alignment tool, the pass-to-pass oscillations are minimized by steering the optical beam on the ring resonator back leg. In particular, the downstream paraboloid is tipped and tilted along with the outcoupler to make the multipass centroids align to the wiggler center line. This procedure had a dramatic effect on FEL startup reliability. It was also found that the multipass alignment had to be done just before lasing as the ring mirrors would drift mechanically and spoil the alignment. This drift would occur if the ring resonator was left unattended for a couple of hours and could be large enough to eliminate all overlap between the pass-to-pass beams. The process then became to bring up the electron beam, size and steer it through the wiggler, perform the multipass alignment of the ring, and search the cavity length for lasing. This was required each time the FEL was operated.

B. Final Lasing Test Results

The culmination of the ring resonator alignment effort occurring in three days of testing is summarized in Table II. As stated above, these results are for an astigmatic resonator, which has been aligned to have its multipass beams overlapping, and the focus positioned near the center of the wiggler. The electron and laser parameters for these three days of operation are listed in the table. The

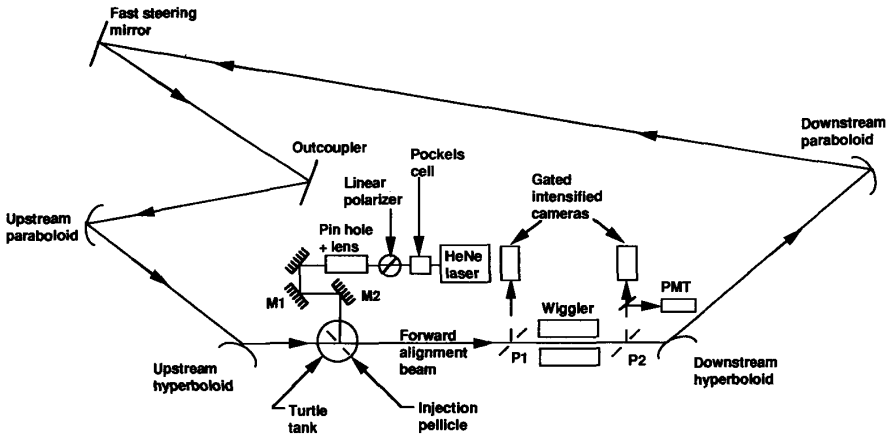

Fig. 10. Schematic drawing of the chopped-pellicle beam alignment system.

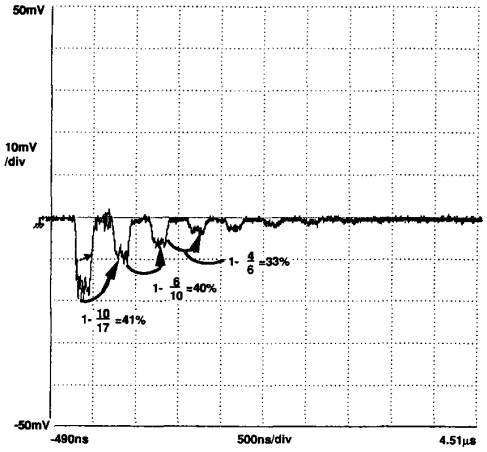

Fig. 11. Ringdown measurement using chopped-pellicle beam and photomultiplier tube (PMT) at sampling pellicle P2. P2 is downstream of the wiggler.

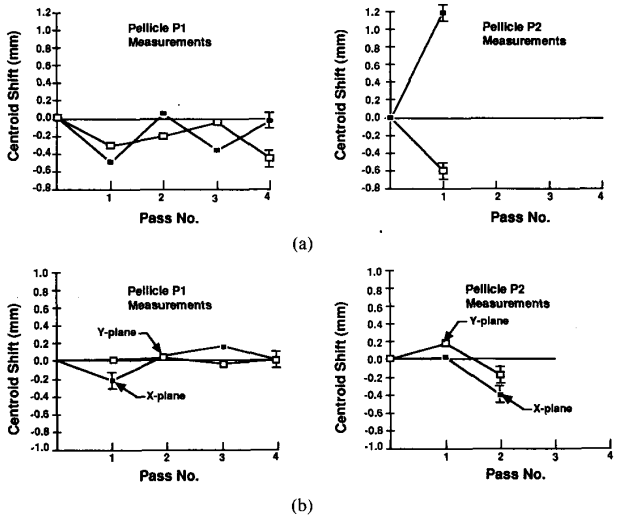

Fig. 12. Gated, intensified camera measurements of the pass-to-pass alignment of the ring resonator. (a) Pass-to-pass alignment before tip/tilts of downstream paraboloid and outcoupler. (b) Pass-to-pass alignment after tip/tilts of downstream paraboloid and outcoupler.

electron beam peak current averaged 195 A with an average edge emittance of 125 π mm · mR. This is the macropulse integrated emittance. The energy slew is defined as the amount the electron beam energy changes during the 110 μs long macropulse.

The optical parameters are also given in Table II. Except for the last day, the wavelength was 635 nm, making the outcoupler transmission 5%. However on October 12, the electron energy was nearly 1 MeV lower, causing the outcoupler transmission to jump to 30%. This significantly higher outcoupling gave larger values for the observed optical energy per micropulse but for a slightly lower extraction efficiency, 0.015% versus 0.028%. This increased outcoupling also caused the ringdown losses to increase from 25 to 50%.

The spectral width on October 12 was also significantly broader than on the two preceding days. If the extraction had been higher, this could have been an early indication of sideband generation. However, this would have required roughly 10 times the observed extraction. Instead it was an electron beam effect. This can be demonstrated by contrasting October 10 and 11 data with October 12 measurements.

Fig. 13 shows the FEL optical output along with electron beam striplines on October 11. This lasing performance was considerably better than the early results presented in Figs. 7 and 8. The newer data exhibit much reduced temporal structure and the extraction is roughly seven times higher. The energy jitter and slew during the macropulse is measured by a stripline in the 180° bend, stripline SL21 [9]. Striplines SL22 and SL23 are in front of the wiggler and give the position and angle changes during the macropulse. The fluttering of the optical intensity at saturation is correlated with variations in the electron beam energy.

TABLE II
ELECTRON BEAM AND LASING DATA FOR OCTOBER 10, 11, AND 12, 1990

	Oct. 10	Oct. 11	Oct.12
Electron Beam			
Energy	109.7	109.7	108.9 MeV
Energy slew	0.25	0.5	0.25%
Micropulse charge (wiggler)	3.1	2.9	3.0 nC
Pulsewidth (injector)	16	15	15 ps
Peak current (wiggler)	197	193	200 A
Normalized edge emittance	($4\epsilon_{rms}$)		
Horizontal plane	107π	117π	149π mm * mR
Vertical plane	168π	122π	115π mm * mR
Energy/micropulse	0.34	0.318	0.327 J
Optical Beam			
Wavelength	637	635	645 nm
Spectral width	2-4	2-4	10-12 nm
Lasing duration	75-80	80-90	90 μs
Ringdown loss	30	25-30	45-50%
Net small-signal gain	35-65	25	50-100%
Energy/micropulse	—	2-8	10-30 μJ
Outcoupler transmission	8	5	30%
Extraction efficiency	—	0.0035-0.028	0.005-0.015%

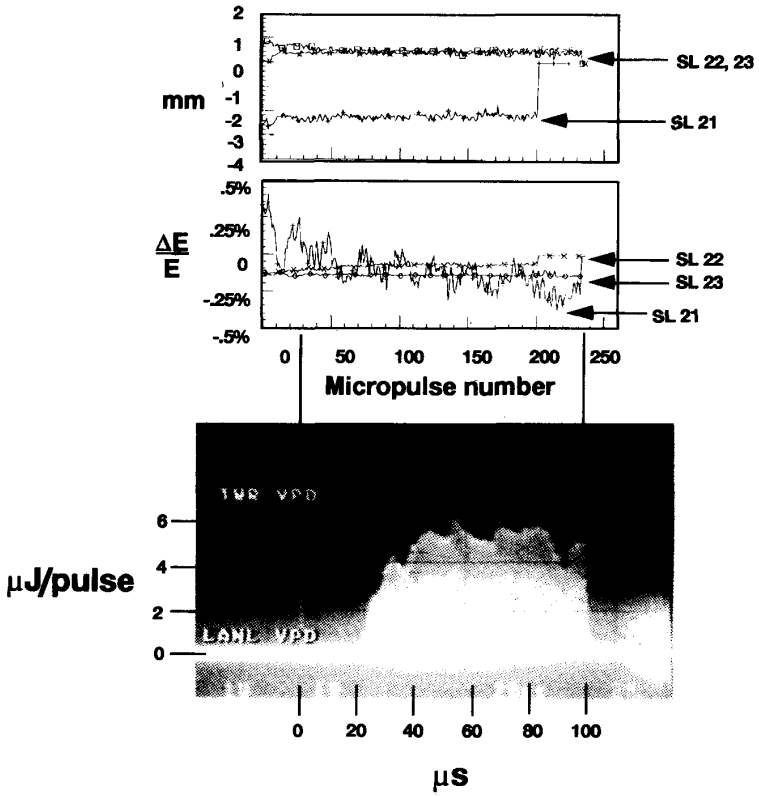

Fig. 13. FEL output and electron beam stripline data for electron energy (SL21) and position (SL22 and SL23) at two locations in front of the wiggler.

The effect of electron energy slew upon lasing wavelength is displayed in Fig. 14 for measurements taken October 12. Here a streak spectrometer image is shown along with the macropulse energy slew measurement. The electron energy slews lower by approximately 0.3% causing the corresponding 0.6% wavelength change. This is expected since the wavelength depends on the square of the electron energy.

The optical output, ringdown loss and net small-signal gain are shown in Fig. 15. The greater optical energy is

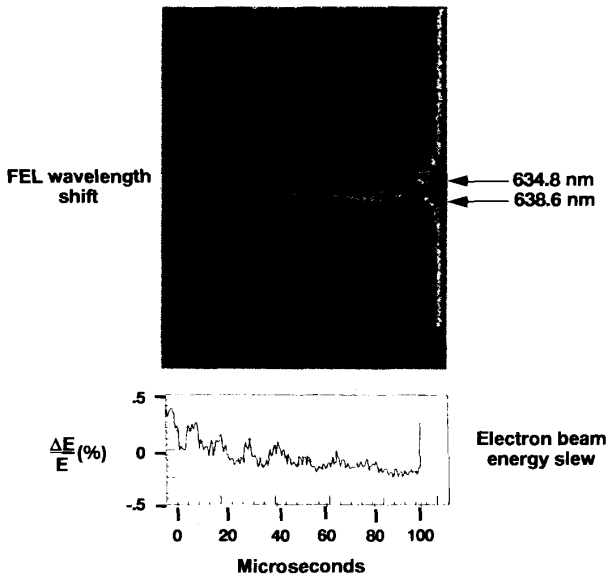

Fig. 14. FEL wavelength shifts agree with electron beam energy slew.

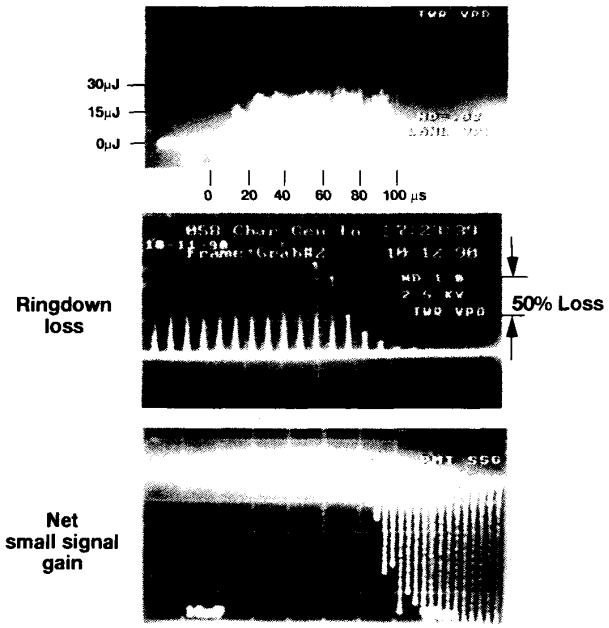

Fig. 15. FEL intensity, ringdown loss, and net small-signal gain for October 12, 1990.

consistent with the increased outcoupling and the higher ringdown loss of 50%. However, the increased outcoupling fraction should not have affected the optical linewidth, which was five times greater on this day. An indication of what was happening could be seen first in the small-signal gain measurement that varies wildly from pass to pass.

A better understanding of what was occurring is obtained from Fig. 16 in which a streak spectrometer image is plotted along with stripline data. The streak spectrometer image shows the spectral evolution of the FEL during the macropulse, time increases to the right, and longer wavelengths are downward in the image. The streak image reveals the source of the 10 to 12 nm linewidth. The wavelength slews around enough during the macropulse to cause the broadening. Comparison with the striplines shows the electron beam had excessively large energy jitter on this day, approximately 0.3% peak to peak. The lower stripline plots are of the vertical and horizontal angular jitter the electron beam has in front of the wiggler. It is interesting that the vertical jitter is larger than the horizontal jitter, but both are well correlated with the energy jitter. This peak-to-peak fast angular fluctuation of 400 μrad is immense for a system that needs to be aligned to a few microns and appears to be the source of both the broadened wavelength and the fluctuating small-signal gain.

C. Electron Beam Quality Considerations

Although much of this paper concerns itself with some of the particular requirements for operating a ring-resonator FEL, it is also important to understand the particular features of using an electron beam as a gain medium. The first and obvious feature is the medium's small volume. The electron beam is essentially a thread, 1 mm in diameter and 5 m long. This string consists of a train of micropulses each being only 3 mm long. Independent of the optical alignment issues of the ring resonator, this electron beam needs to be precisely aligned along the full 5 m wiggler length to 10 μm in both the transverse and longitudinal dimensions. The beam is also required to have low energy spread and be stable on the scale of the ponderomotive bucket size, roughly 0.1% in energy and a fraction of a picosecond. Failure to achieve any of these parameters will cause the FEL to either operate at a drastically reduced lasing intensity, exhibit structured output, or not lase at all.

Therefore, during all the tests described here and those preceding them, it was essential to develop electron beam instrumentation and improve the accelerator and beamline to achieve as many of the above requirements as possible. It should be noted that most of the effects observed and discussed experimentally are principally due to either electron beam or optical cavity phenomena. It is only after these technical problems are solved that the FEL physics can be done.

V. Summary and Conclusion

The initial results of operating a FEL with a grazing-incidence ring resonator exhibited a structured optical output, and startup was unreliable. Measurements were performed to separate electron beam and ring-resonator effects. Calculations showed that startup problems were likely due to poor resonator alignment, whereas the structured lasing intensity was dominated by fluctuations in the electron beam. Therefore, efforts were made to develop

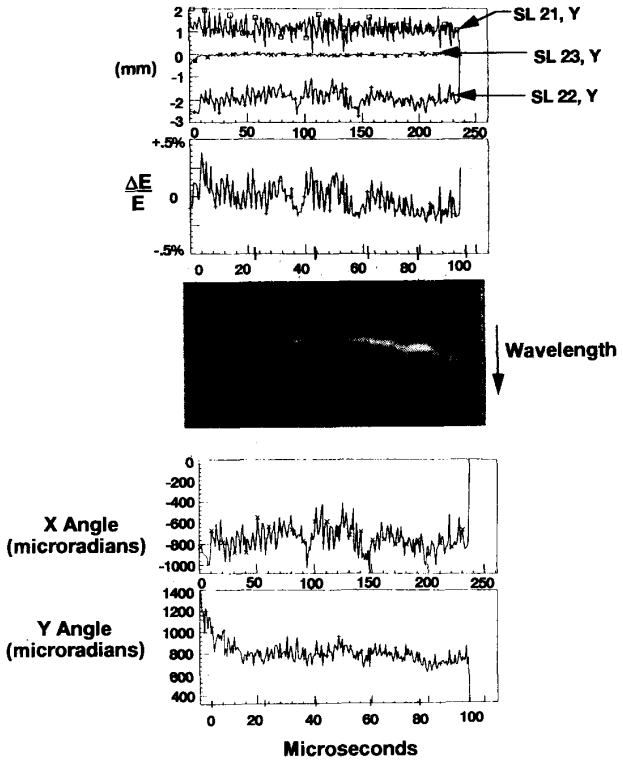

Fig. 16. Streak camera image of wavelength versus time with electron beam energy, position, and angle stripline measurements.

an additional alignment laser producing a chopped beam to quantify the resonator's walking mode. This chopped beam not only clearly demonstrated the presence of the pass-to-pass walking behavior but also provided a means for correcting it by tipping the downstream paraboloid and the outcoupler flat. Renewed testing with the aligned, but still astigmatic, resonator resulted in reliable operation and a sevenfold increase in the extraction efficiency.

The next step was to remove the astigmatism, increase the bandwidth of the stabilization system, and upgrade the electron accelerator. This work was nearing completion when the direction of the FEL project changed, and the ring resonator experiment was discontinued. However, this decision was not the result of any fundamental technical shortcomings of using a grazing-incidence ring resonator with an FEL. The change was instead motivated by the desire to redirect limited resources toward a true average power FEL [16]. Therefore, the results presented here do not represent the capabilities of a fully optimized ring-resonator free-electron laser.

Acknowledgment

It is impossible to imagine making a device as complicated as an FEL work without the efforts of talented and dedicated people. The authors thank P. Johnson, K. McCrary, M. Bemes, R. Hawkins, and A. Currie for building, maintaining, and operating the FEL; L. Milliman and C. Lancaster for software support; and M. Bailey and D. Schultz for installing and maintaining the various optical systems. There were also useful discussions with A. Vetter, R. Kennedy, T. Buller, L. Tyson, and A. D. Yeremian. We also received helpful advice from J. Slater, K. Robinson, D. Quimby, and D. Shemwell. These are the people who made it work.

References

[1] A. H. Lumpkin, R. L. Tokar, D. H. Dowell, A. R. Lowrey, A. D. Yeremian, and R. E. Justice, "Improved performance of the Boeing/LANL FEL experiment, extraction efficiency and cavity length detuning effects," *Nuclear Instrum. Methods*, vol. A296, pp. 169–180, 1990.

[2] S. V. Benson, W. S. Fann, B. A. Hooper, J. M. J. Madey, E. B. Szarmes, B. Richman, and L. Vintro, "A review of the Stanford Mark III FEL program," *Nuclear Instrum. Methods*, vol. A296, pp. 110–114, 1990.

[3] J. M. Eggleston, "Angularity stable ring resonators for high power FEL's," in *Proc.*, Int. Conf. on Lasers. McLean, VA: STS Press, 1985, p. 305.

[4] S. V. Gunn and K. C. Sun, "Design of a ring resonator for burst mode free electron laser," in *Proc.*, AIAA 19th Fluid Dynam., Plasma Dynam. Laser Conf., Honolulu, HI, 1987, paper AIAA-87-1280.

[5] B. D. McVey, "Three-dimensional simulations of free electron laser physics," *Nuclear Instrum. Methods*, vol. A250, pp. 449–455, 1986.

[6] J. Goldstein, private communication.

[7] R. L. Tokar, B. D. McVey, L. E. Thode, and G. M. Gallatin, "Simulations of a ring resonator free electron laser," *IEEE J. Quantum Electron.*, vol. 25, pp. 73–83, 1989.

[8] A. D. Yeremian, J. Adamski, R. Kennedy, W. Gallagher, J. Orthel,

and L. Young, "Boeing 120 MeV RF Linac injector design and accelerator performance comparison with PARMELA," in *Proc.*, IEEE Par. Accel. Conf., Chicago, IL, 1989, pp. 657-659.

[9] D. H. Dowell, M. L. Laucks, A. R. Lowrey, M. Bemes, A. Currie, P. Johnson, K. McCrary, A. Adamski, D. R. Shoffstall, A. H. Lumpkin, and R. L. Tokar, "Improved electron beam quality of the Boeing free electron laser," *Nucl. Instrum. Methods*, vol. A304, pp. 336-341, 1991.

[10] M. L. Laucks, D. H. Dowell, A. R. Lowrey, M. Bemes, A. Currie, P. Johnson, K. McCrary, J. Adamski, D. Pistoresi, D. R. Shoffstall, M. Bentz, R. Burns, R. Hydyma, K. Sun, W. Mower, R. Tokar, A. H. Lumpkin, S. Bender, B. McVey, J. Goldstein, and D. Shemwell, "Optical measurements of the Boeing free electron laser," *Nucl. Instrum. Methods*, vol. A304, pp. 25-30, 1991.

[11] R. Hudyma and L. Eigler, "Computer-aided alignment of a grazing incidence ring resonator for a visible wavelength free electron laser," in *Proc. SPIE*, Int. Lens Design Conf., vol. 1354, pp. 523-532, June 1990.

[12] C. E. Knapp, V. K. Viswanathan and Q. D. Appert, "Analysis of the Boeing FEL mirror measurements," presented at SPIE Meet. of Opt., Electro-Opt. and Laser Applicat. in Sci. and Engineer., Los Angeles, CA, Jan. 15-20, 1989.

[13] K. L. Brown "TRANSPORT computer program for electron beam optics," Stanford Linear Accelerator Laboratory, Report No. SLAC-75.

[14] D. H. Dowell, J. Adamski, A. R. Lowrey, and A. H. Lumpkin, "Phase-space matching in a five meter wiggler using optical transition radiation," *Nuclear Instrum. Methods*, vol. A296, pp. 315-357, 1990.

[15] R. L. Tokar, L. M. Young, A. H. Lumpkin, B. D. McVey, L. E. Thode, S. C. Bender, K. C. D. Chan, A. D. Yeremian, D. H. Dowell, A. R. Lowrey, and D. C. Quimby, "INEX simulations of the Boeing FEL system," *Nuclear Instrum. Methods*, vol. A296, pp. 115-126, 1990.

[16] C. G. Parazzoli, R. E. Rodenburg, J. B. Romero, J. L. Adamski, D. J. Pistoresi, D. R. Shoffstall, and D. C. Quimby, "CW 100 kW radio frequency free electron laser design at 10 μm," *IEEE J. Quantum Electron.*, this issue, pp. 2605-2612.

David H. Dowell received the M.S. and Ph.D. degrees from the University of Illinois, Urbana, in 1974 and 1981, respectively.

His interest in accelerator physics began during undergraduate study while writing computer codes for the design of an electron microtron at the University of Illinois. He later obtained the Ph.D. degree in experimental nuclear physics using the beam from this same accelerator. From 1981 to 1983 he continued post-doctoral studies in nuclear physics at the University of Washington, Seattle. In Fall 1983, he became a staff physicist at Brookhaven National Laboratory, Upton, NY. While at Brookhaven, he participated in research at the Tandem Van de Graff Facility, University of Illinois, and University of Mainz, Germany, and planned experiments for the Laser Electron Gamma Source facility then under construction at the National Synchrotron Light Source. This facility produces polarized high energy gamma ray beams by the Compton back scattering of laser light from the storage ring electron beam. Since 1987, he has been with the Boeing FEL Facility, Seattle, WA.

Mary L. Laucks received the B.S. degree from the University of California, Santa Barbara, in physics and the M.S. degree from the University of Washington, Seattle, also in physics, in 1980 and 1985, respectively.

From 1980 to 1981 she was with the Santa Barbara Research Center where she tested IR detector arrays. She worked on Boeing's free-electron laser program from 1987 to 1991. She was involved in the instrumentation of electron beam diagnostics, the design of optical diagnostics for the ring resonator, and the initial laser tests with the ring resonator.

A. R. Lowrey, photograph and biography not available at the time of publication.

John L. Adamski, photograph and biography not available at the time of publication.

Denis J. Pistoresi, for a biography, see this issue, p. 2612.

Donald R. Shoffstall, photograph and biography not available at the time of publication.

Melvin Paul Bentz received the A.A. degree in 1971.

He has worked in a variety of different fields in research and development for the past seven years. More recently, during the past three years, with Rockwell Power Systems, Albuquerque, NM. He worked on the installation, alignment, maintenance, and test of various high-energy lasers including the RACHL chemical laser, EMRLD excimers, and the Boeing free-electron laser.

Richard H. Burns received the B.S. and M.E. degrees from Cornell University, Ithica, NY, in 1967 and 1968, respectively.

He was with the Jet Propulsion Lab designing celestial sensors for spacecraft navigation and at the Librascope Division of the Singer Company developing laser-driven displays. Since 1982 he has conducted research on high-energy lasers at the Rocketdyne Division of Rockwell International, Canoga Park, CA. He is credited with six patents in the field of optics.

Jay Guha received the M.A. and Ph.D. degrees in physics from University of Southern California, Los Angeles, in 1972 and 1973, respectively.

His areas of interest include spectroscopy, nonlinear optics, laser diagnostics, and electrooptics. He was a postdoctoral scholar at the University of Michigan, Ann Arbor, and an Assistant Professor at the University of Toledo, OH. During his seven years at Rockwell International, he has been working on various aspects of resonator concepts, laser diagnostics, resonator alignment, and alignment control.

Kenneth C. Sun received the B.S. degree from the Massachusetts Institute of Technology, Cambridge, and the M.S. degree from the University of Washington, Seattle, both in aeronautics and astronautics, in 1977 and 1978, respectively.

From 1979 to 1981, he was with the Lockheed Missiles and Space Co. and worked on various high-energy laser (HEL) beam control systems from LODE, Talon Gold, and SLCSAT. In July 1981, he joined Rocketdyne's Advanced Optical System group and worked on various HEL resonators for free-elelctron lasers, chemical oxygen-iodine lasers, xenon-fluoride excimer lasers, and HF/DF chemical lasers. He was the Chief Scientist for all Rocketdyne resonator subcontracts with Boeing's free-electron laser program. He was heavily involved in the design, fabrication, and installation of the uncooled grazing-incidence ring resonator discussed herein.

William Tomita received the B.S.E.E. degree from the University of California, Berkeley, and the M.S.E.E. degree from the University of Southern California, Los Angeles.

His involvement with lasers started in 1962 while he was with the Hughes Aircraft Co. Since then, he has worked on various laser-related programs such as microimage recording on inorganic, organic, and metallic thin films and rangefinding and target designations systems. After joining Rocketdyne in 1988, he performed the initial coarse alignment of the Burst Mode ring resonator at BREL in 1989.

A. H. Lumpkin, photograph and biography not available at the time of publication.

S. C. Bender, photograph and biography not available at the time of publication.

D. Byrd, photograph and biography not available at the time of publication.

Robert L. Tokar, photograph and biography not available at the time of publication.